

Defending Unauthorized Model Merging via Dual-Stage Weight Protection

Wei-Jia Chen¹ Min-Yan Tsai¹ Cheng-Yi Lee² Chia-Mu Yu¹

¹ National Yang Ming Chiao Tung University

² Independent Researcher

{wer9u623, chengyi.lee.1224, chiamuyu}@gmail.com

Abstract

The rapid proliferation of pretrained models and open repositories has made model merging a convenient yet risky practice, allowing free-riders to combine fine-tuned models into a new multi-capability model without authorization. Such unauthorized model merging not only violates intellectual property rights but also undermines model ownership and accountability. To address this issue, we present MERGEWARD, a proactive dual-stage weight protection framework that disrupts merging compatibility while maintaining task fidelity. In the first stage, we redistribute task-relevant information across layers via L_2 -regularized optimization, ensuring that important gradients are evenly dispersed. In the second stage, we inject structured perturbations to misalign task subspaces, breaking curvature compatibility in the loss landscape. Together, these stages reshape the model’s parameter geometry such that merged models collapse into destructive interference while the protected model remains fully functional. Extensive experiments on both vision (ViT-L-14) and language (Llama2, Gemma2, Mistral) models demonstrate that MERGEWARD reduces merged model accuracy by up to 90% with less than 1.5% performance loss on the protected model.

1. Introduction

The pretrain–finetune paradigm has become a cornerstone of modern AI, where large pretrained models are efficiently adapted to downstream domains through lightweight finetuning. This workflow, widely adopted in vision [11], language [1, 33], and multimodal [28] communities, has been further catalyzed by open repositories such as Hugging Face [39], GitHub [13], and ModelScope [25], which host thousands of publicly available checkpoints. Developers can now easily obtain and recombine high-quality models without additional training. Among these techniques, model merging [44], which integrates multiple finetuned models derived from the same pretrained source via parameter-level composition, has become a practical means

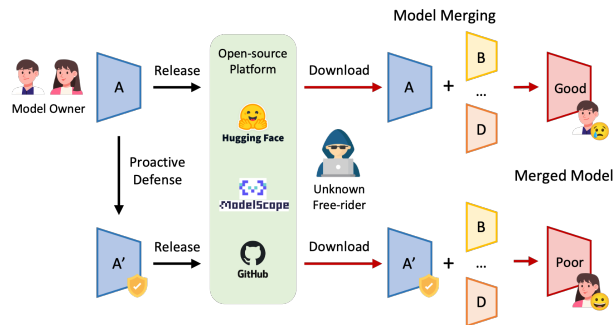


Figure 1. Unauthorized model merging and its defense.

to construct multi-task or cross-domain models [45].

However, this openness also introduces a growing intellectual property risk [9, 43]. Free-riders can download fine-tuned models released under specific license terms and merge them to create new multi-capability models for redistribution or commercial use without authorization. Because parameter blending inherently conceals the provenance of individual weights, such *unauthorized model merging* [18] allows the resulting model to inherit specialized capabilities without reproducing the original training cost or respecting licensing restrictions, posing significant challenges to model ownership [35] and attribution [21].

To mitigate this threat, we propose a *proactive* defense that preprocesses the model’s parameters so that any subsequent merging will degrade functionality while preserving the model’s own task performance. Designing such a defense, however, faces two key challenges. First, the defender can only modify the parameters of their own model and cannot anticipate the attacker’s model, merging strategy, or target tasks, making the defense highly uncertain. Second, the defender must simultaneously maintain the model’s original accuracy and suppress the merged model’s effectiveness under the constraint of controlling only their own parameters (see Figure 1).

We make an observation that recent advances [16, 40, 42, 48] in model merging often rely on sparsification [27, 47],

which aims to distribute task-specific information across different layers and weights before merging. By sparsifying each fine-tuned model, their task-relevant parameters become less overlapping in the parameter space, reducing interference when the two models are later combined. Consequently, the merged model can largely retain the capabilities of each constituent model.

Building on the above observation, we introduce a defensive two-stage preprocessing strategy, MERGEWARD, to disrupt unauthorized model merging. The key idea is to reshape the model’s weight distribution so that merging no longer preserves task performance. Specifically, we first *redistribute* the parameter values, spreading those originally concentrated in a few high-magnitude weights across a wider set of parameters. This dispersal maintains the model’s functionality on its original task but makes the merging process unstable, as the diffused weights are more easily amplified, diluted, or interfered with during parameter blending. However, simple averaging alone cannot fully resist merging. To further reinforce protection, we selectively adjust influential parameters by applying controlled perturbations. Because task-relevant knowledge has already been dispersed across many smaller weights, this targeted manipulation minimally affects the standalone model but substantially degrades the performance of any merged version. Through this dual adjustment, MERGEWARD effectively preserves the integrity of the protected model while inducing collapse in unauthorized merged models.

To validate the robustness of MERGEWARD, we consider two adaptive attacks. The first attempts to neutralize the defense by subtracting a scaled copy of the protected model’s parameters from the merged weights. The second aims to estimate the hidden disturbance vector and project each gradient update orthogonally to it, avoiding movement along the defended direction during retraining. However, both strategies fail to undermine our defense (see Section 7).

MERGEWARD has shown high effectiveness on a variety of tasks and architectures. For ViT-L-14 on the GTSRB and MNIST, the accuracy of the preprocessed model only decreased slightly (less than 1%). However, after merging, the accuracy of GTSRB plummeted from 86.78% to 12.19%, and MNIST from 96.02% to 11.35%. For large language models (LLMs), the accuracy after merging generally dropped to single digits, with some even falling to 0%. For example, the accuracy of the Gemma2 decreased from 69.6% to 1.52% on the GSM8K after merging, and from 64.02% to 21.34% on the HumanEval.

Contributions. Our contributions are shown below:

- We propose MERGEWARD, a proactive defense that redistributes and perturbs model weights to prevent unauthorized merging while preserving task performance.
- Experiments on ViT-L-14, Llama2, Gemma2, and Mistral show that MERGEWARD reduces merged

model accuracy by up to 90% with less than 1.5% loss on the protected model.

- We evaluate two adaptive attacks and show that both fail to circumvent the defense due to dispersed task information and unobservable perturbations.

2. Related Works

Model Merging. Model merging is a training-free method for combining multiple fine-tuned models into a single multi-task model by directly manipulating their parameters. Through techniques such as weight averaging (WA) [40], the parameters of several models can be linearly combined to produce a new model capable of handling multiple tasks simultaneously. Task arithmetic (TA) [16] further interprets tasks as vectors in the parameter space, enabling addition or subtraction between task representations. Other approaches, including TIES [4] and DARE [48], enhance merging quality via parameter sparsity and sign consistency, achieving better interpretability without additional data. More recent studies [6, 10, 12, 24, 46] extend these ideas to broader architectures and scenarios, developing increasingly flexible and efficient merging strategies.

Defenses against Unauthorized Model Merging. To the best of our knowledge, PaRaMS [18] is the only work that proactively defends against unauthorized model merging. In particular, PaRaMS introduces parameter rearrangement and random multi-head scaling: the former reorders MLP parameters, and the latter randomly scales attention heads while maintaining functional equivalence, thereby pushing the model out of the shared parameter basin and significantly degrading the merged model’s performance by slightly harming the original task accuracy.

3. Background Knowledge on Model Merging

Let θ_{pre} denote the parameters of the pre-trained model, and θ_i the parameters of a fine-tuned model on task \mathcal{D}_i . For n task-specific models $\theta_1, \dots, \theta_n$ derived from the same pre-trained model θ_{pre} , model merging can be formulated as $\theta_{\text{merge}} = \text{Merge}(\theta_{\text{pre}}, \theta_1, \dots, \theta_n)$, where Merge represents a specific parameter-level fusion strategy.

Task Arithmetic (TA). TA [16] assumes that the task-specific update from θ_{pre} to θ_i encodes the distinctive capability of task \mathcal{D}_i . This update, referred to as the *task vector* $\tau_i = \theta_i - \theta_{\text{pre}}$, can be linearly combined across tasks to obtain $\theta_{\text{merge}} = \theta_{\text{pre}} + \lambda \sum_i \tau_i$, where λ controls the merging scale. TA therefore constructs a multi-task model by directly superposing these task vectors.

TIES-Merging. Extending TA, TIES-merging [42] aims to alleviate interference between tasks caused by redundant or conflicting parameters. It first trims each task vector τ_i by retaining only the top- $k\%$ parameters with the largest magnitudes, then elects a unified parameter sign across tasks,

and finally performs a disjoint merge that averages only the parameters consistent with the selected sign. This three-step procedure improves stability and reduces destructive interference in the merged model.

AdaMerging. AdaMerging [46] introduces an adaptive and unsupervised model merging framework that automatically learns task-wise or layer-wise coefficients without using original training data. By minimizing prediction entropy on unlabeled samples, it adjusts merging weights to balance task contributions, thereby improving multi-task performance, generalization, and robustness. This adaptive strategy can be integrated with TA or TIES-merging to further enhance merging quality and stability.

4. System Model

Attack Scenario. We consider a common scenario in which a *defender* fine-tunes a large pretrained model θ_{pre} on a domain-specific dataset to achieve high task performance and subsequently releases the model θ_{def} to the community. A *free-rider*, however, may download this open-sourced model and merge it with another model under their control. We assume that the free-rider’s model, θ_{fr} , is also fine-tuned from the same pretrained model θ_{pre} , a typical setup in current practice since most finetuning pipelines start from public backbones. By merging the two models, the free-rider seeks to inherit the defender’s specialized capabilities at minimal cost and combine them with their own model’s functionality. The defender’s goal is therefore to proactively modify its model θ_{def} so that it remains fully functional on the intended task but loses effectiveness when merged with any other model.

Free-rider’s Capability. The free-rider is assumed to have limited computational resources, making expensive retraining or knowledge distillation [15, 36] infeasible. In particular, because the free-rider is highly cost-sensitive, they will not perform knowledge distillation on T_{def} even though the dataset is downloadable, as such retraining still incurs substantially higher computation and tuning costs compared to direct parameter merging. Instead, they rely on low-cost model merging as a shortcut to acquire the defender’s expertise. The free-rider has full white-box access to the defender’s released model and a task-specific model θ_{fr} derived from the same θ_{pre} . The attack is considered successful if the merged model θ_{merge} achieves accuracy comparable to θ_{def} on the defender’s task T_{def} while preserving its own performance on T_{fr} , where T_X denotes X ’s domain-specific task.

Defender’s Capability. The defender has full access to and control over the parameters of their own model θ_{def} and can apply parameter-level transformations to strengthen protection. These modifications must maintain the model’s original task performance while preventing the merged model from retaining it. Although the defender cannot access the

free-rider’s model, it can reasonably assume both originate from the same model θ_{pre} ; otherwise, merging would not be feasible [6, 10, 12, 16, 24, 40, 46]. A successful defense ensures that the released model remains fully functional for legitimate use but any merged version experiences a substantial accuracy drop on T_{def} .

Problem Setup. The free-rider’s goal is to construct a merged model $\theta_{\text{merge}} = \text{Merge}(\theta_{\text{pre}}, \theta_{\text{def}}, \theta_{\text{fr}})$ that simultaneously satisfies $\text{Perf}(\theta_{\text{merge}}, T_{\text{def}}) \approx \text{Perf}(\theta_{\text{def}}, T_{\text{def}})$ and $\text{Perf}(\theta_{\text{merge}}, T_{\text{fr}}) \approx \text{Perf}(\theta_{\text{fr}}, T_{\text{fr}})$, where $\text{Merge}(\cdot)$ denotes a parameter-level fusion method such as model soups or task arithmetic [6, 10, 12, 16, 24, 40, 46], and $\text{Perf}(\cdot)$ represents the appropriate utility metric for the target model family (e.g., accuracy for vision or perplexity for language models). To counter this, the defender instead releases a protected model $\hat{\theta}_{\text{def}} = \text{Defense}(\theta_{\text{def}})$ whose standalone performance remains intact, $\text{Perf}(\hat{\theta}_{\text{def}}, T_{\text{def}}) \approx \text{Perf}(\theta_{\text{def}}, T_{\text{def}})$, but any merged version $\hat{\theta}_{\text{merge}} = \text{Merge}(\theta_{\text{pre}}, \hat{\theta}_{\text{def}}, \theta_{\text{fr}})$ exhibits a pronounced degradation, $\text{Perf}(\hat{\theta}_{\text{merge}}, T_{\text{def}}) \ll \text{Perf}(\theta_{\text{def}}, T_{\text{def}})$. Hence, our objective is to design a proactive defense function $\text{Defense}(\cdot)$ that enforces this degradation property while maintaining the protected model’s utility on its intended task.

5. Proposed Method

To address unauthorized merging, we propose MERGE-GUARD, which comprises two stages: ① Density-Aware Finetuning (training stage) and ② Adversarial Weight Negation (training-free stage). We first outline the key idea behind MERGEGUARD, then describe each stage in detail.

Key Idea. As discussed in Section 3, most of recent model merging techniques such as TIES [42] and AdaMerging [46] rely on sparsification to distribute task-relevant parameters sparsely across layers, reducing interference and enabling merged models to preserve multiple capabilities.

As shown in Figure 2, MERGEGUARD builds on this observation from a defensive perspective. In the first stage, *Density-Aware Finetuning* disperses task-critical weights through L_2 -regularized training, ensuring that important information is evenly spread across layers rather than concentrated in a few parameters. This dispersed structure provides stability for the second stage, *Adversarial Weight Negation*, which selectively offsets a subset of task-relevant directions to intentionally misalign them with potential merging counterparts. Because the weight importance has already been evenly distributed by *Stage 1*, these perturbations preserve the model’s own task performance while disrupting the cross-model compatibility required for successful merging. Together, the two stages reshape the parameter landscape so that merging attempts result in destructive interference, effectively neutralizing unauthorized model combina-

tion.

Stage 1: Density-Aware Finetuning. The goal of this stage is to disperse task-critical weights across different layers through training. In addition to the standard cross-entropy loss L_{CE} used in classification, we introduce an L_2 regularization term that drives model parameters toward zero, encouraging a more balanced distribution of important information. The overall loss can be expressed as:

$$L_{\text{total}} = L_{\text{CE}} + \alpha L_2, \quad (1)$$

where α is a hyperparameter that balances L_{CE} and L_2 . For vision models, the loss takes the form $L_{\text{total}} = -\sum_{t=1}^T y_t \log(\hat{y}_t) + \alpha \sum_{\ell=1}^L \|\theta^{(\ell)}\|_2^2$, where $L_{\text{CE}} = -\sum_{t=1}^T y_t \log(\hat{y}_t)$ and $L_2 = \sum_{\ell=1}^L \|\theta^{(\ell)}\|_2^2$. Here, y_t denotes the ground-truth label of the t -th class, \hat{y}_t the predicted probability, and $\theta^{(\ell)}$ the trainable parameters of layer ℓ . The L_2 penalty is applied independently to each layer.

For LLMs, the loss is written as:

$$L_{\text{total}} = -\sum_{t=1}^T \log P(y_t | y_{<t}, x; \theta) + \alpha \sum_{\ell=1}^L \|\theta^{(\ell)}\|_2^2, \quad (2)$$

where $P(y_t | y_{<t}, x; \theta)$ is the conditional probability of predicting token y_t given the previous context $y_{<t}$. This formulation applies L_2 regularization to each layer's parameters, smoothing large-magnitude weights and evenly distributing task-relevant signals across the network.

Overall, given θ_{def} , we obtain θ'_{def} after *Stage 1*. By reducing the concentration of dominant weights, this stage effectively disperses important information throughout the model, making subsequent merging operations less stable and thereby diminishing the merged model's performance.

Stage 2: Adversarial Weight Negation. This stage introduces a training-free procedure that intentionally offsets task-relevant weights to disrupt merging compatibility. We begin by masking each layer of the model and measuring the resulting accuracy drop. The top $k\%$ of layers that cause the largest performance degradation are identified as critical and excluded from subsequent operations.

Afterwards, a binary masking vector M is then constructed, where elements corresponding to $k\%$ critical layers and to the least significant $(1-k)(1-k')\%$ parameters are set to zero, and those in the remaining $k(1-k')\%$ range are set to one. This selective preservation ensures that later weight adjustments do not damage essential functionality.

Next, we calculate

$$\hat{\theta}_{\text{def}} = \theta'_{\text{def}} - \beta M \odot \tau'_{\text{def}}, \quad (3)$$

where \odot denotes the inner product, $\tau'_{\text{def}} = \theta'_{\text{def}} - \theta_{\text{pre}}$ denotes the task vector representing the direction of the defender's fine-tuning, and $\beta > 0$ is a small perturbation

factor. Subtracting τ_{def} in the masked parameter space weakens certain informative directions without compromising the core task performance. Consequently, the protected model remains stable on its own task, but any merged version suffers severe degradation due to misaligned task directions and dilution introduced by the merging algorithm.

We particularly note that some layers differ drastically in parameter scale across tasks, and directly applying this operation can destabilize the model. To prevent such collapse in LLMs, we exclude three layers, *model.embed.tokens.weight*, *model.norm.weight*, and *lm_head.weight*, from the subtraction process, while ViT-based models undergo the full operation.

Theoretical Justification of MERGEGUARD. Model merging can be expressed as a parameter-level combination:

$$\theta_{\text{merge}} = \theta_{\text{pre}} + \lambda_1(\theta_{\text{def}} - \theta_{\text{pre}}) + \lambda_2(\theta_{\text{fr}} - \theta_{\text{pre}}), \quad (4)$$

where $\lambda_1, \lambda_2 \in [0, 1]$ control the blending ratio. A successful merge implicitly assumes that both task vectors $\tau_{\text{def}} = \theta_{\text{def}} - \theta_{\text{pre}}$ and $\tau_{\text{fr}} = \theta_{\text{fr}} - \theta_{\text{pre}}$ reside in a *shared linear subspace* representing compatible gradient directions [31, 37, 49]. In this case, their superposition still corresponds to a descent direction in the loss landscape [3, 22], preserving both tasks.

MERGEGUARD breaks this assumption by jointly modifying both the *magnitude distribution* and the *directional alignment* of τ_{def} . Formally, after *Stage 1*, the finetuned parameters become $\theta'_{\text{def}} = \theta_{\text{pre}} + \tau'_{\text{def}}$, where $\tau'_{\text{def}} = \tau_{\text{def}} + \epsilon$, $\mathbb{E}[\epsilon] = 0$, and $\text{Cov}[\epsilon] = \sigma^2 I$. This step redistributes task-relevant gradients isotropically, flattening the curvature of the local basin and ensuring that important information is evenly spread rather than concentrated along a few dominant directions. Consequently, the Hessian eigenvectors associated with large eigenvalues, those that previously spanned the shared merging subspace, become decorrelated and dispersed.

Then, *Stage 2* injects a small but structured perturbation along a *locally adversarial* direction: $\hat{\theta}_{\text{def}} = \theta'_{\text{def}} - \beta M \odot \tau'_{\text{def}}$ (Eq. 3). This operation effectively rotates the task vector by an angle $\phi = \arccos \frac{\langle \tau'_{\text{def}}, \tau_{\text{fr}} \rangle}{\|\tau'_{\text{def}}\| \|\tau_{\text{fr}}\|}$, thereby increasing the expected interference term in the merged loss:

$$\Delta \mathcal{L}_{\text{merge}} \approx \lambda_1 \lambda_2 \|\tau'_{\text{def}}\| \|\tau_{\text{fr}}\| (1 - \cos \phi), \quad (5)$$

which grows quadratically with the misalignment angle. In practice, even small rotations (e.g., $\phi > 30^\circ$) suffice to push the merged model outside the shared basin, causing the loss landscape to exhibit destructive interference between the two task vectors. As the masked perturbation preserves low-order statistics within each critical layer, the standalone model maintains its original functionality, while any linear

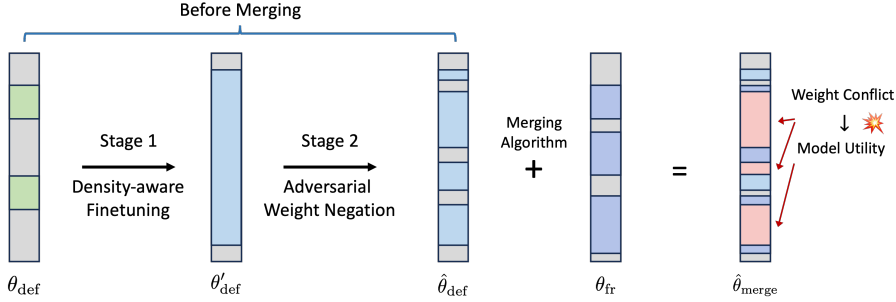


Figure 2. The workflow of MERGEWARD.

or sparsity-based fusion [6, 10, 12, 16, 24, 40, 46, 48] collapses due to incompatible curvature directions.

Hence, MERGEWARD’s defense can be theoretically interpreted as *inducing curvature misalignment* in the task subspace, transforming the previously compatible manifold of fine-tuned models into disjoint basins. This ensures that the merged parameter θ_{merge} no longer lies near a stationary point of either task’s loss function, leading to substantial degradation in unauthorized merged models.

6. Evaluation

6.1. Experiment Setups

Models. For the image classification task, we adopt the ViT-L-14 [11] architecture, a transformer-based vision backbone widely used for downstream adaptation. For image generation, we employ Stable Diffusion 1.5 (SD1.5) [29], a latent diffusion model trained on large-scale text–image pairs. For the language tasks, we evaluate three representative architectures: Llama2-7B [33], Gemma2-9B [32], and Mistral-7B [17].

Datasets. For image classification, we evaluate across eight diverse datasets: SUN397 [41], Cars [19], RESISC45 [5], SVHN [26], GTSRB [30], MNIST [20], EuroSAT [14], and DTD [7], which span natural scenes, fine-grained objects, digits, satellite imagery, and textures. For image generation, we consider WikiArt [38] and Naruto [2]. For LLM evaluation, we employ AlpacaEval [23] for instruction following, GSM8K [8] for mathematical reasoning, and HumanEval [4] for program synthesis. Details about these datasets are shown in the Appendix.

Metrics. In image classification, we report top-1 accuracy to assess recognition capability. For LLMs, the AlpacaEval benchmark reports the win rate against Zephyr-7B [34]; the GSM8K benchmark measures the proportion of correctly solved problems; and the HumanEval benchmark measures pass@1 accuracy [4], indicating the fraction of valid programs that pass all test cases.

Merging Methods. We assess the robustness of MERGEWARD under multiple representative model-merging paradigms, including Weight Averaging (WA) [40], Task

Arithmetic (TA) [16], TIES-Merging (TIES) [42], and AdaMerging (ADA) [46], with DARE [48] additionally employed as an optional pre-processing module to form DT (DARE+TIES) used in LLMs.

Baselines. Following prior work, PaRaMS [18] serves as the only proactive defense specifically designed against unauthorized model merging. Hence, we use PaRaMS as the sole baseline for quantitative comparison.

Implementation of MERGEWARD. In our implementation, the *Density-Aware Finetuning* stage requires no additional hyperparameter tuning. The *Adversarial Weight Negation* stage introduces two hyperparameters, k' and k , controlling the proportion of preserved and perturbed layers, respectively. Unless otherwise stated, we set $k' = 10$ and $k = 0.1$ throughout all experiments. α in Eq. 1 is 0.01 and β in *Stage 2* is set to 1 in our experiments. The merging coefficients are determined by each model merging methods [16, 40, 42, 46, 48].

Table 1. Standalone model accuracy before/after MERGEWARD.

	SUN397	Cars	RESISC45	EuroSAT	SVHN	GTSRB	MNIST	DTD
θ_{pre}	68.24	77.94	71.33	62.72	58.45	50.55	76.36	55.37
θ_{def}	82.32	92.39	97.37	99.81	98.11	99.24	99.69	84.15
$\hat{\theta}_{\text{def}}$	81.52	8829	97.25	95.46	96.82	98.25	99.27	82.16

6.2. Experimental Results

6.2.1. Results on Image Classification

Table 1 summarizes the classification accuracy of θ_{pre} , θ_{def} , and $\hat{\theta}_{\text{def}}$. As expected, fine-tuning θ_{pre} on T_{def} substantially improves performance, confirming the effectiveness of task adaptation. Comparing θ_{def} with $\hat{\theta}_{\text{def}}$, we observe that MERGEWARD maintains nearly identical accuracy, introducing only a negligible drop, which demonstrates that the protection process preserves the model’s original utility.

Table 2 summarizes the image classification results on MERGEWARD under different model merging methods. Across all evaluated merging paradigms, MERGEWARD consistently enforces significant degradation on the merged models while preserving the original model’s performance.

Table 2. Classification accuracy of the merged models without MERGEWARD (θ_{merge}) and with MERGEWARD ($\hat{\theta}_{\text{merge}}$).

Method	SUN397		Cars		RESISC45		EuroSAT		SVHN		GTSRB		MNIST		DTD	
	θ_{merge}	$\hat{\theta}_{\text{merge}}$														
WA [40]	72.1	56.16	81.6	76.63	82.6	4.98	91.9	13.07	78.2	10.05	70.7	44.28	97.1	38.97	62.8	2.61
TA [16]	73.9	54.27	82.1	38.24	86.6	56.50	94.1	54.94	87.9	47.28	86.7	12.91	98.9	11.35	65.6	46.65
TIES [42]	76.5	70.77	85.0	45.64	89.3	33.51	95.7	14.48	90.3	7.77	83.3	4.44	99.0	35.70	68.6	48.88
ADA [46]	79.4	65.51	90.3	74.19	91.6	72.27	97.4	11.22	93.4	7.76	97.5	2.19	99.0	71.37	79.2	49.20

Table 3. The comparison between MERGEWARD and PaRaMS [18]. Each number corresponds to the classification accuracy (%). The average accuracy drop is 30.76 for PaRaMS and is 52.11 for MERGEWARD.

Methods	SUN397		Cars		RESISC45		EuroSAT		SVHN		GTSRB		MNIST		DTD	
	θ_{def}	$\hat{\theta}_{\text{merge}}$														
PaRaMS [18]	82.32	56.77	92.39	38.61	97.37	67.86	99.81	74.81	98.11	71.95	99.24	52.25	99.69	96.02	84.15	48.72
MERGEWARD	81.52	54.27	88.29	38.24	97.25	56.50	95.46	54.94	96.82	47.28	98.25	12.91	99.27	11.35	82.16	46.65

In particular, the preprocessing causes only a marginal reduction (typically less than 1%) in standalone accuracy, indicating that the dual-stage mechanism minimally affects the base model’s functionality. However, once the protected models are merged, their accuracy drops drastically across all datasets. Compared to the unprotected or baseline configurations, MERGEWARD achieves much larger post-merge degradation across all merging strategies.

Table 3 summarizes the image classification results comparing MERGEWARD with PaRaMS [18]. During the preprocessing stage, MERGEWARD introduces a minor accuracy drop on the original model due to the regularization and perturbation applied in the protection process. In contrast, PaRaMS [18], which only performs parameter rearrangement, preserves the original accuracy almost perfectly. However, after model merging, the gap between the two defenses becomes substantial. MERGEWARD consistently enforces stronger degradation on the merged models while maintaining near-original accuracy on the protected model. For instance, on GTSRB and MNIST, MERGEWARD in TA reduced the original accuracy by less than 2%, yet the merged accuracy dropped sharply from 86.78% to 12.91% and from 98.94% to 11.35%, respectively. By comparison, PaRaMS only reduced the same metrics to 52.25% and 96.02%. These results confirm that MERGEWARD substantially weakens merging compatibility.

6.2.2. Results on Image Generation

Figure 3 illustrates the qualitative comparison on Stable Diffusion 1.5. We use Naruto as the defender’s task (T_{def}) and WikiArt as the free-rider’s task (T_{fr}). The first two columns visualize the images generated by θ_{def} and θ_{fr} , respectively. When tested with prompts A_0 and A_1 designed for Naruto, the free-rider’s model θ_{fr} can also reproduce the character, indicating that it has captured the semantic style of Naruto. The merged model θ_{merge} , obtained through standard parameter fusion, inherits this capability and suc-

cessfully generates Naruto-style images, demonstrating a clear case of intellectual property leakage.

In contrast, under MERGEWARD, the protected standalone model θ_{def} still preserves its generative fidelity and produces faithful Naruto imagery. However, the protected merged model $\hat{\theta}_{\text{merge}}$ fails to reproduce the Naruto character, yielding only partially coherent but semantically mismatched results. This degradation confirms that MERGEWARD effectively prevents the unauthorized inheritance of generative capabilities while preserving the original model’s usability.

6.2.3. Results on Text Classification

Figure 4 presents the performance of MERGEWARD on LLMs under various merging strategies. Across all benchmarks, the protected models maintain comparable accuracy prior to merging. However, once merged, their performance degrades sharply. For instance, both Llama2 and Mistral experience nearly a 50% drop in overall accuracy, while Gemma2 suffers even more severe degradation. On the GSM8K benchmark, which evaluates mathematical reasoning, the merged models become almost non-functional, showing frequent calculation errors and skipped reasoning steps, with accuracy often falling to single-digit levels (e.g., Mistral with TA drops from 75.7% to 0%). Similarly, on the HumanEval code generation task, MERGEWARD consistently reduces post-merge pass@1 accuracy by more than half. Qualitative inspection further reveals that many generated programs, though sometimes passing test cases, contain redundant or looping code segments, as illustrated in the Appendix.

6.3. Ablation Studies

To evaluate the contribution of each stage in MERGEWARD, we compare the effects of applying *Stage 1*, *Stage 2*, and their combination (*Stage 1 + 2*). Table 4 reports the performance of the ViT-L/14 across multiple datasets,



Figure 3. Visualization Results of SD 1.5.

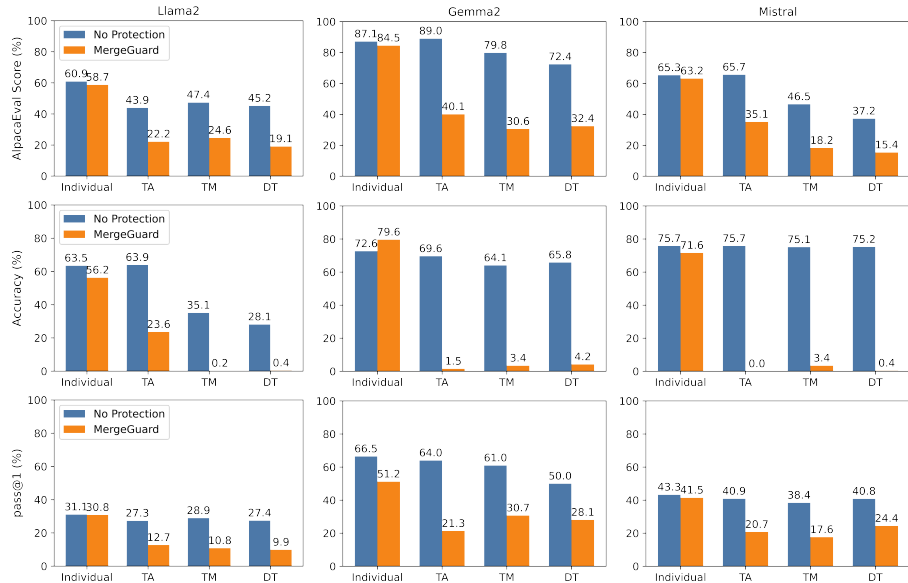


Figure 4. Overall comparison across benchmarks and models. Each row corresponds to a benchmark (AlpacaEval for instruction-following, GSM8K for reasoning, and HumanEval for code generation), and each column corresponds to a model (Llama2, Gemma2, Mistral). Orange and blue bars denote results with and without MERGEGUARD, respectively.

Table 4. The results of ablation study. Each number indicates classification accuracy (%).

Method	SUN397		Cars		RESISC45		EuroSAT		SVHN		GTSRB		MNIST		DTD	
	$\hat{\theta}_{\text{def}}$	$\hat{\theta}_{\text{merge}}$														
Stage I	79.96	76.38	90.79	72.25	93.48	85.38	98.07	75.06	97.29	81.21	98.37	12.21	99.30	13.37	81.77	63.60
Stage II	80.10	75.94	92.10	77.33	92.74	75.33	99.83	79.79	98.11	77.88	99.25	64.86	99.73	83.60	80.16	54.20
Stage I + II	79.14	54.27	88.29	38.24	92.16	56.50	95.46	54.94	96.82	47.28	98.25	12.91	99.27	11.35	80.08	46.65

where it shows baseline accuracy before applying any protection, and presents results after each protection configuration. We observe that although the standalone stages cause a similar minor accuracy drop before merging, their combination (*Stage 1 + 2*) leads to a much larger degradation in the merged model’s accuracy. This indicates that the two stages complement each other: *Stage 1* disperses task-relevant weights to stabilize the model, while *Stage 2*

exploits this dispersed structure to misalign merging directions effectively.

6.4. Discussion

Why MERGEGUARD Outperforms PaRaMS in Image/Text Classification. Compared with PaRaMS, which relies solely on deterministic parameter rearrangement and random multi-head scaling, MERGEGUARD’s two-stage

process produces more structured disruption in task-space geometry. In image and text classification, tasks are dominated by discriminative gradients that occupy relatively low-dimensional subspaces. MERGEGUARD’s weight redistribution amplifies the sensitivity of these subspaces to cross-task interference: the dispersed small weights contribute collectively to stable single-task performance but amplify destructive interference under linear merging, leading to a steeper accuracy collapse than PaRaMS. From a loss landscape perspective [3, 22], MERGEGUARD reshapes each classifier’s basin into multiple narrow valleys separated by sharp ridges, while PaRaMS merely translates the basin position. Thus, the merged model under MERGEGUARD lands closer to the curvature apex (high loss), producing stronger merging degradation.

Why $\hat{\theta}_{\text{merge}}$ Cannot Generate Random Noise. As discussed in Section 6.2.2, the MERGEGUARD-protected merged model $\hat{\theta}_{\text{merge}}$ fails to reproduce the defender’s task T_{def} but does not completely collapse into random noise. In contrast, the PaRaMS-protected merged model often outputs pure noise patterns. Both defenses achieve equivalent levels of intellectual property protection, neither reveals task-specific visual traits from T_{def} , yet the perceptual outcomes differ significantly.

This discrepancy stems from how each method disrupts representational continuity in generative models. Diffusion-based generators depend on smooth manifold alignment between latent and pixel spaces. PaRaMS introduces random multi-head scaling and parameter rearrangement, which destroy such continuity, leading to decorrelated feature channels and complete breakdown of generative structure. In contrast, MERGEGUARD perturbs model parameters in a structured manner: its L_2 -regularized redistribution preserves weak weight correlations that maintain partial coherence in the latent manifold. Thus, MERGEGUARD prevents semantic fidelity without inducing total noise collapse.

In essence, PaRaMS enforces representational incoherence across generative layers, while MERGEGUARD enforces functional incompatibility within discriminative subspaces. Hence, PaRaMS is more disruptive for continuous generative pipelines (e.g., diffusion models), whereas MERGEGUARD is better suited for discriminative or classification-oriented tasks where decision-boundary misalignment is the primary defense objective.

7. Adaptive Attack

The free-rider may be aware of the deployment of MERGEGUARD and could develop adaptive attacks to circumvent it. We consider two such adaptive attacks, UNMASK and GRADEERASE, described below.

UNMASK. The design rationale behind UNMASK is to neutralize the defensive perturbation introduced by MERGEGUARD by directly subtracting the protected model’s pa-

Table 5. Evaluation of different adaptive attacks.

	SUN397	Cars	RESISC45	EuroSAT	SVHN	GTSRB	MNIST	DTD	Avg.
θ_{pre}	68.24	77.94	71.33	62.72	58.45	50.55	76.36	55.37	65.12
θ_{merge}	73.90	82.10	86.60	94.10	87.90	86.70	98.90	65.60	84.47
$\hat{\theta}_{\text{merge}}$	54.27	38.24	56.50	54.94	47.28	12.91	11.35	46.65	40.26
UNMASK	67.75	71.19	68.35	64.44	68.71	51.50	71.79	53.46	64.64
GRADEERASE	67.36	71.58	76.60	64.10	54.08	14.58	10.28	55.60	51.77

rameters from the merged weights. Specifically, the free-rider constructs an adaptive model $\theta_{\text{Unmask}} = \text{Merge}(\theta_{\text{pre}}, \hat{\theta}_{\text{def}}, \theta_{fr}) - \lambda \cdot \hat{\theta}_{\text{def}}$, where λ follows the scaling factor used in TA (0.3 in our experiments).

GRADEERASE. GRADEERASE is designed to counteract MERGEGUARD by removing the gradient component aligned with the defender’s hidden perturbation direction. Specifically, the free-rider estimates the disturbance vector $v_{\text{disturb}} = -\tau_G$ from limited training data and modifies each gradient update as $g' = g - \frac{\langle g, v_{\text{disturb}} \rangle}{\|v_{\text{disturb}}\|^2} v_{\text{disturb}}$, thereby eliminating the defensive direction during retraining.

Summary of Adaptive Attacks. For UNMASK, although subtracting the protected model’s parameters can partially neutralize MERGEGUARD’s perturbations, it concurrently removes essential task-specific information, causing the merged model’s performance on T_{def} to regress to the pretrained level T_{pre} , as shown in Table 5. In contrast, GRADEERASE projects each gradient update orthogonally to the estimated disturbance vector v_{disturb} , thereby avoiding reinforcement of the defended direction. However, because the estimation of v_{disturb} is inherently noisy and incomplete, this attack fails to fully restore merging compatibility.

Overall, as summarized in Table 5, MERGEGUARD reduces the merged accuracy from 84.47 to 40.26 on average. Although UNMASK and GRADEERASE can partially recover the merged model to 64.64 and 51.77, respectively, MERGEGUARD still maintains a substantial degradation margin of at least 20% across all tasks. This demonstrates that even under adaptive settings, MERGEGUARD remains effective in preventing the merged model from achieving functional usability.

8. Conclusion

We presented MERGEGUARD, a dual-stage defense that proactively prevents unauthorized model merging. By redistributing and adversarially perturbing task-relevant weights, MERGEGUARD disrupts curvature alignment in the loss landscape, making merged models collapse while preserving the original task performance. Extensive experiments show up to 90% degradation in merged accuracy with minimal impact on the protected model. Compared to PaRaMS, MERGEGUARD achieves stronger resistance in discriminative tasks, revealing that shaping weight geometry, not just rearranging parameters, is key to safeguarding model ownership.

References

[1] Tom Brown, Benjamin Mann, Nick Ryder, Melanie Subbiah, Jared D Kaplan, Prafulla Dhariwal, Arvind Neelakantan, Pranav Shyam, Girish Sastry, Amanda Askell, et al. Language models are few-shot learners. *NeurIPS*, 33:1877–1901, 2020. 1

[2] Eole Cervenka. Naruto blip captions. <https://huggingface.co/datasets/lambdalabs/naruto-blip-captions/>, 2022. Accessed: 2025-11-12. 5

[3] Huanran Chen, Yinpeng Dong, Zeming Wei, Yao Huang, Yichi Zhang, Hang Su, and Jun Zhu. Unveiling the basin-like loss landscape in large language models. *arXiv preprint arXiv:2505.17646*, 2025. 4, 8

[4] Mark Chen. Evaluating large language models trained on code. *arXiv preprint arXiv:2107.03374*, 2021. 2, 5

[5] Gong Cheng, Junwei Han, and Xiaoqiang Lu. Remote sensing image scene classification: Benchmark and state of the art. *Proceedings of the IEEE*, 105(10):1865–1883, 2017. 5

[6] Jiho Choi, Donggyun Kim, Chanhyuk Lee, and Seunghoon Hong. Revisiting weight averaging for model merging. *arXiv preprint arXiv:2412.12153*, 2024. 2, 3, 5

[7] Mircea Cimpoi, Subhransu Maji, Iasonas Kokkinos, Sammy Mohamed, and Andrea Vedaldi. Describing textures in the wild. In *CVPR*, pages 3606–3613, 2014. 5

[8] Karl Cobbe, Vineet Kosaraju, Mohammad Bavarian, Mark Chen, Heewoo Jun, Lukasz Kaiser, Matthias Plappert, Jerry Tworek, Jacob Hilton, Reiichiro Nakano, et al. Training verifiers to solve math word problems. *arXiv preprint arXiv:2110.14168*, 2021. 5

[9] Tianshuo Cong, Delong Ran, Zesen Liu, Xinlei He, Jinyuan Liu, Yichen Gong, Qi Li, Anyu Wang, and Xiaoyun Wang. Have you merged my model? on the robustness of large language model ip protection methods against model merging. In *Proceedings of the 1st ACM Workshop on Large AI Systems and Models with Privacy and Safety Analysis*, pages 69–76, 2023. 1

[10] Pala Tej Deep, Rishabh Bhardwaj, and Soujanya Patra. Della-merging: Reducing interference in model merging through magnitude-based sampling. *arXiv preprint arXiv:2406.11617*, 2024. 2, 3, 5

[11] Alexey Dosovitskiy. An image is worth 16x16 words: Transformers for image recognition at scale. *arXiv preprint arXiv:2010.11929*, 2020. 1, 5

[12] Guodong Du, Junlin Lee, Jing Li, Runhua Jiang, Yifei Guo, Shuyang Yu, Hanting Liu, Sim K Goh, Ho-Kin Tang, Daojing He, et al. Parameter competition balancing for model merging. *NeurIPS*, 37:84746–84776, 2024. 2, 3, 5

[13] GitHub. Github repository. <https://github.com>, 2025. Accessed: 2025-11-12. 1

[14] Patrick Helber, Benjamin Bischke, Andreas Dengel, and Damian Borth. Eurosat: A novel dataset and deep learning benchmark for land use and land cover classification. *IEEE Journal of Selected Topics in Applied Earth Observations and Remote Sensing*, 12(7):2217–2226, 2019. 5

[15] Geoffrey Hinton, Oriol Vinyals, and Jeff Dean. Distilling the knowledge in a neural network. *arXiv preprint arXiv:1503.02531*, 2015. 3

[16] Gabriel Ilharco, Marco Tulio Ribeiro, Mitchell Wortsman, Ludwig Schmidt, Hannaneh Hajishirzi, and Ali Farhadi. Editing models with task arithmetic. In *ICLR*, 2023. 1, 2, 3, 5, 6

[17] Albert Q. Jiang, Alexandre Sablayrolles, Arthur Mensch, Chris Bamford, Devendra Singh Chaplot, Diego de las Casas, Florian Bressand, Gianna Lengyel, Guillaume Lampe, Lucile Saulnier, Lélio Renard Lavaud, Marie-Anne Lachaux, Pierre Stock, Teven Le Scao, Thibaut Lavril, Thomas Wang, Timothée Lacroix, and William El Sayed. Mistral 7b, 2023. 5

[18] Wei Junhao, Yu Zhe, and Jun Sakuma. Disrupting model merging: A parameter-level defense without sacrificing accuracy. In *ICCV*, pages 17698–17707, 2025. 1, 2, 5, 6

[19] Jonathan Krause, Michael Stark, Jia Deng, and Li Fei-Fei. 3d object representations for fine-grained categorization. In *ICCV Workshops*, pages 554–561, 2013. 5

[20] Yann LeCun. The mnist database of handwritten digits. <http://yann.lecun.com/exdb/mnist/>, 1998. 5

[21] Dongfang Li, Zetian Sun, Xinshuo Hu, Zhenyu Liu, Ziyang Chen, Baotian Hu, Aiguo Wu, and Min Zhang. A survey of large language models attribution. *arXiv preprint arXiv:2311.03731*, 2023. 1

[22] Hao Li, Zheng Xu, Gavin Taylor, Christoph Studer, and Tom Goldstein. Visualizing the loss landscape of neural nets. *NeurIPS*, 31, 2018. 4, 8

[23] Xuechen Li, Tianyi Zhang, Yann Dubois, Rohan Taori, Ishaan Gulrajani, Carlos Guestrin, Percy Liang, and Tat-sunori B Hashimoto. Alpacaeval: An automatic evaluator of instruction-following models, 2023. 5

[24] Zhenyi Lu, Chenghao Fan, Wei Wei, Xiaoye Qu, Dangyang Chen, and Yu Cheng. Twin-merging: Dynamic integration of modular expertise in model merging. *NeurIPS*, 37:78905–78935, 2024. 2, 3, 5

[25] ModelScope. Modelscope: Open-source model platform. <https://modelscope.cn/>, 2025. Accessed: 2025-11-12. 1

[26] Yuval Netzer, Tao Wang, Adam Coates, Alessandro Bissacco, Baolin Wu, Andrew Y Ng, et al. Reading digits in natural images with unsupervised feature learning. In *NeurIPS Workshop on deep learning and unsupervised feature learning*, page 7. Granada, 2011. 5

[27] Binhang Qi, Hailong Sun, Wenrui Long, Ruobing Zhao, Xiang Gao, et al. Cabs: Conflict-aware and balanced sparsification for enhancing model merging. In *ICML*, 2025. 1

[28] Alec Radford, Jong Wook Kim, Chris Hallacy, Aditya Ramesh, Gabriel Goh, Sandhini Agarwal, Girish Sastry, Amanda Askell, Pamela Mishkin, Jack Clark, et al. Learning transferable visual models from natural language supervision. In *ICML*, pages 8748–8763. PMLR, 2021. 1

[29] Robin Rombach, Andreas Blattmann, Dominik Lorenz, Patrick Esser, and Björn Ommer. High-resolution image synthesis with latent diffusion models. In *CVPR*, pages 10684–10695, 2022. 5

[30] Johannes Stallkamp, Marc Schlipsing, Jan Salmen, and Christian Igel. The german traffic sign recognition benchmark: a multi-class classification competition. In *IJCNN*, pages 1453–1460. IEEE, 2011. 5

[31] Derek Tam, Mohit Bansal, and Colin Raffel. Merging by matching models in task parameter subspaces. *Transactions on Machine Learning Research (TMLR)*, 2024. 4

[32] Gemma Team, Morgane Riviere, Shreya Pathak, Pier Giuseppe Sessa, Cassidy Hardin, Surya Bhupatiraju, Léonard Hussonot, Thomas Mesnard, Bobak Shahriari, Alexandre Ramé, et al. Gemma 2: Improving open language models at a practical size. *arXiv preprint arXiv:2408.00118*, 2024. 5

[33] Hugo Touvron, Louis Martin, Kevin Stone, Peter Albert, Amjad Almahairi, Yasmine Babaei, Nikolay Bashlykov, Soumya Batra, Prajjwal Bhargava, Shruti Bhosale, et al. Llama 2: Open foundation and fine-tuned chat models. *arXiv preprint arXiv:2307.09288*, 2023. 1, 5

[34] Lewis Tunstall, Edward Emanuel Beeching, Nathan Lambert, Nazneen Rajani, Kashif Rasul, Younes Belkada, Shengyi Huang, Leandro Von Werra, Clémentine Fourrier, Nathan Habib, et al. Zephyr: Direct distillation of lm alignment. In *COLM*, 2024. 5

[35] Lixu Wang, Shichao Xu, Ruiqi Xu, Xiao Wang, and Qi Zhu. Non-transferable learning: A new approach for model ownership verification and applicability authorization. In *ICLR*, 2022. 1

[36] Tianyu Wang, Jianzong Wang, Shiliang Zhang, and Jing Xiao. A survey of knowledge distillation: Techniques, applications and outlook. *IEEE Trans. Neural Networks and Learning Systems.*, 34(3):1231–1249, 2023. 3

[37] Yongxian Wei, Anke Tang, Li Shen, Chun Yuan, and Xiaochun Cao. Modeling multi-task model merging as adaptive projective gradient descent. In *ICML*, 2025. 4

[38] WikiArts. Wikiarts captions. https://huggingface.co/datasets/fusing/wikiart_captions, 2025. Accessed: 2025-11-12. 5

[39] Thomas Wolf, Lysandre Debut, Victor Sanh, Julien Chau- mond, Clement Delangue, Anthony Moi, Pierrick Cistac, Tim Rault, Rémi Louf, Morgan Funtowicz, et al. Huggingface’s transformers: State-of-the-art natural language processing. *arXiv preprint arXiv:1910.03771*, 2019. 1

[40] Mitchell Wortsman, Gabriel Ilharco, Samir Ya Gadre, Rebecca Roelofs, Raphael Gontijo-Lopes, Ari S Morcos, Hongseok Namkoong, Ali Farhadi, Yair Carmon, Simon Kornblith, et al. Model soups: averaging weights of multiple fine-tuned models improves accuracy without increasing inference time. In *ICML*, pages 23965–23998. PMLR, 2022. 1, 2, 3, 5, 6

[41] Jianxiong Xiao, James Hays, Krista A Ehinger, Aude Oliva, and Antonio Torralba. Sun database: Large-scale scene recognition from abbey to zoo. In *CVPR*, pages 3485–3492. IEEE, 2010. 5

[42] Prateek Yadav, Derek Tam, Leshem Choshen, Colin A Raffel, and Mohit Bansal. Ties-merging: Resolving interference when merging models. *NeurIPS*, 36:7093–7115, 2023. 1, 2, 3, 5, 6

[43] Shojiro Yamabe, Futa Kai Waseda, Tsubasa Takahashi, and Koki Wataoka. MergePrint: Merge-resistant fingerprints for robust black-box ownership verification of large language models. In *Proceedings of the 63rd Annual Meeting of the Association for Computational Linguistics (Volume 1: Long Papers)*, pages 6894–6916. Association for Computational Linguistics, 2025. 1

[44] Enneng Yang, Li Shen, Guibing Guo, Xingwei Wang, Xiaochun Cao, Jie Zhang, and Dacheng Tao. Model merging in llms, mllms, and beyond: Methods, theories, applications and opportunities. *arXiv preprint arXiv:2408.07666*, 2024. 1

[45] Enneng Yang, Li Shen, Zhenyi Wang, Guibing Guo, Xiaojun Chen, Xingwei Wang, and Dacheng Tao. Representation surgery for multi-task model merging. In *ICML*, pages 56332–56356, 2024. 1

[46] Enneng Yang, Zhenyi Wang, Li Shen, Shiwei Liu, Guibing Guo, Xingwei Wang, and Dacheng Tao. Adamerging: Adaptive model merging for multi-task learning. In *ICLR*, 2024. 2, 3, 5, 6

[47] Yan Yang, Yixia Li, Hongru Wang, Xuetao Wei, James Jianqiao Yu, Yun Chen, and Guanhua Chen. Impart: Importance-aware delta-sparsification for improved model compression and merging in llms. In *Proceedings of the 63rd Annual Meeting of the Association for Computational Linguistics (Volume 1: Long Papers)*, pages 18817–18829, 2025. 1

[48] Le Yu, Bowen Yu, Haiyang Yu, Fei Huang, and Yongbin Li. Language models are super mario: Absorbing abilities from homologous models as a free lunch. In *ICML*, 2024. 1, 2, 5

[49] Luca Zhou, Daniele Solombrino, Donato Crisostomi, Maria Sofia Bucarelli, Giuseppe Alessio D’Inverno, Fabrizio Silvestri, and Emanuele Rodolà. On task vectors and gradients. *arXiv preprint arXiv:2508.16082*, 2025. 4